Multiphoton-Injected Plasmas in InSb

R. E. SLUSHER, W. GIRIAT,* AND S. R. J. BRUECK†
Bell Telephone Laboratories, Murray Hill, New Jersey 07974
(Received 2 December 1968)

Electron-hole plasmas injected in InSb by irradiation with an intense CO_2 laser beam are studied. These plasmas result from multiphoton production of electron-hole pairs in pure InSb samples. The density, homogeneity, recombination radiation, and conductivity of these injected plasmas were observed at 77 and 4.2°K in external magnetic fields from 0 to 55 kOe. It is found that homogeneous plasma densities of 10^{15} cm^{-3} can be produced over a 1-mm cube. Possible mechanisms for plasma lifetimes are discussed. Interesting properties and applications of the multiphoton-injected plasma are suggested.

I. INTRODUCTION

THE high-intensity Q-switched CO_2 laser has made it possible to inject dense electron-hole plasmas in narrow band gap semiconductors by multiphoton absorption.[1] These plasmas are interesting because they are field-free, are as cold as the lattice, and can be produced in very pure, intrinsic materials. InSb is of particular interest, because it exists in very pure single crystals (n or $p\sim5\times10^{13}$/cm^3), and because plasmas injected into it by other means have been shown to exhibit many interesting instabilities.[2] The injected plasmas can be studied by observing their photoconductivity,[3] optical absorption, recombination radiation,[1] and light scattering. We have used the first three methods to study the plasma density, homogeneity, and the magnetic field dependence of the conductivity and recombination radiation.

There are several unique advantages of the multiphoton plasma injection technique. The relatively low multiphoton absorption coefficients allow the creation of plasma throughout the bulk of the semiconductor crystal. In InSb we show that a homogeneous plasma can be generated in a 1 mm^3 volume with a density of 10^{15}/cm^3. The spacial position of the plasma is controlled by the focused laser beam. The plasma density can be controlled by the laser intensity. Multiphoton-injected plasmas can be probed by small electric fields, a method not applicable for high electric field injection techniques.[2] The recombination radiation from the injected plasmas show that they are in equilibrium with the lattice at temperatures as low as 10°K. Plasmas at these low temperatures are difficult or impossible to obtain by other techniques. The multiphoton plasmas can also be injected in high magnetic fields.[3] However, the creation rate is field-dependent because of the variation of the band energies in a magnetic field. Since there is no need for contacts required for electric field injection, problems of impurities, heating, and homogeneity of the contact surface are eliminated. Finally, the CO_2 laser beam used to produce the plasma can also be used to study the properties of the plasma. Inelastic scattering of the incident laser beam can be used to study the Landau and spin levels in a magnetic field,[4] the optic and acoustic plasma modes,[5,6] and the Doppler-shifted single-particle velocity distribution.[7] This scattering technique should yield particularly interesting results near plasma instability.[8,9]

Several interesting experiments which should be possible because of the unique properties listed above have been suggested by Wolff.[10] In a very low density plasma the electrons and holes may form an insulating gas of bound excitons. As the density increases the excitons begin to overlap and a transition occurs to a conducting state. This is the well-known Mott transition.[11] The large exciton radius ($a\sim6\times10^{-6}$ cm) makes the insulating phase unlikely in InSb in zero field. However, as a magnetic field is applied the exciton radius perpendicular to the field decreases. Freeze-out to the donor sites has been observed at 2.5°K in fields above 50 kOe.[4] A similar freeze-out to the excitonic insulating state should be possible in the multiphoton-injected plasma. Other experiments suggested by Wolff include giant density waves in the ground state of the plasma[13,14] and the two-stream instability.[15] Another interesting possibility is the observation of the acoustic plasmon by light scattering. In doped semiconductors the acoustic plasmon is severely damped by electron-impurity collisions. Since the multiphoton plasmas can

* Present address: Institute of Physics, Warsaw, Poland.
† Present address: Electrical Engineering Department, MIT, Cambridge, Mass.
[1] C. K. N. Patel, P. Fleury, R. Slusher, and H. Frisch, Phys. Rev. Letters **16**, 971 (1966).
[2] Betsy Ancker-Johnson, in *Semiconductors and Semimetals*, edited by R. K. Willardson and A. C. Beer (Academic Press Inc., New York, 1966), Vol. I.
[3] K. J. Button, B. Lax, M. H. Weiler, and M. Reine, Phys. Rev. Letters **17**, 1005 (1966).
[4] R. E. Slusher, C. K. N. Patel, and P. A. Fleury, Phys. Rev. Letters **18**, 77 (1967).
[5] C. K. N. Patel and R. E. Slusher, Phys. Rev. **167**, 413 (1968).
[6] B. Tell and R. J. Martin, Phys. Rev. **167**, 381 (1968).
[7] A. Mooradian, Phys. Rev. Letters **20**, 1102 (1968).
[8] P. M. Platzman, Phys. Rev. **139**, A379 (1965).
[9] S. Ishimaru, D. Pines, and N. Rostoker, Phys. Rev. Letters **8**, 231 (1962).
[10] Private communication.
[11] The Mott transition has recently been observed in single-photon-injected plasmas in Ge; see V. M. Asnin and A. A. Rogachev, Zh. Eksperim. i Teor Fiz. Pis'ma v Redaktsiyu **7**, 464 (1968) [English transl.: Soviet Phys.—JETP Letters **7**, 360 (1968)].
[12] O. Beckman, E. Hanamura, and L. J. Neuringer, Phys. Rev. Letters **18**, 773 (1967).
[13] V. Celli and N. D. Mermin, Phys. Rev. **140**, A839 (1965).
[14] P. A. Wolff, J. Phys. Chem. Solids **27**, 685 (1966).
[15] O. Buneman, Phys. Rev. Letters **1**, 8 (1958).

be injected in pure materials this obstacle may be side-stepped. Plasma lifetimes, as a function of density and magnetic field, is still another area of interest.

In this paper we describe a number of basic preliminary experiments on the multiphoton-injected plasma in InSb. It has been shown[16] and confirmed by our experiments that at zero field the predominant injection mechanism for the CO_2 laser is two-photon absorption, as described by Braunstein[17] and Keldysh.[18] This mechanism is independent of sample orientation and is stronger than the generation and absorption of second harmonics produced by bound electrons, which depends strongly on sample orientations. The two-photon creation rate is of the order of[1]

$$W_L \sim 5\times 10^8 E_L^4 \text{ cm}^{-3} \text{ sec}^{-1}, \quad (1)$$

where E_L (in V/cm) is the electric field of the focused laser, which is typically of the order of 10^4 V/cm. If the densities of the injected electrons, n, and holes, p, are greater than 10^{14} cm^{-3}, the trapping levels[19] are probably saturated and the density of the free-electron–hole plasma should be determined by the bimolecular radiative recombination rate τ_R ($\sim 10^{-8}$ sec for InSb; see Sec. II B). Thus, during the quasi-equilibrium period near the peak of the laser pulse, the maximum plasma density is expected to be of the order of

$$n \gtrsim (5\times 10^{24}\times \tau_R) \text{ cm}^{-3} \approx 5\times 10^{16} \text{ cm}^{-3} \quad (2)$$

for $E_L \approx 10^4$ V/cm, which corresponds to an intensity $I \approx 5\times 10^5$ W/cm^2. The two-photon absorption coefficient is of the order of

$$\alpha \simeq 10^{-20} E_L^4 \text{ cm}^{-1}, \quad (3)$$

(E_L in V/cm), which is much smaller than the hole absorption,

$$\alpha \sim 5\times 10^{-15} p \text{ cm}^{-1} \quad (4)$$

(p in cm^{-3}) for hole densities larger than 10^{14} cm^{-3}. Thus, the attenuation of the laser and homogeneity of the plasma are limited by the hole absorption. First we will describe some measurements of the plasma density and homogeneity and then discuss the variation of conductivity and recombination radiation with magnetic field.

II. EXPERIMENTAL RESULTS

A. General Apparatus

A rotating mirror Q-switched CO_2 laser was used to produce 5–10-kW peak power for 0.3-μsec pulses with a repetition rate of 120 Hz. Dielectric filters were used to separate the 9.6- and 10.6-μ radiation emitted by the laser. The InSb samples were n- and p-type material with concentrations of $\sim 5\times 10^{13}$ and 10^{14} cm^{-3}, respectively. Samples were in the form of polished bars or plates which were maintained on shielded cold fingers or in direct contact with liquid nitrogen and helium. Irtran II windows sealed with epoxy admitted the laser radiation into the liquid chamber.

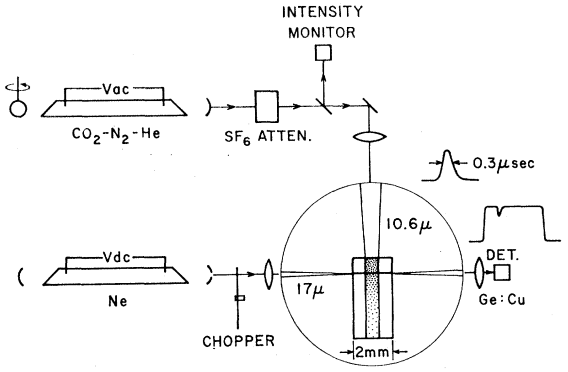

FIG. 1. Diagram of experimental apparatus for measuring density and homogeneity of two-photon-injected plasma in InSb. Enlarged diagram within the circle shows the injecting and measuring laser beams.

B. Intensity Dependence of Density and Homogeneity

The density and homogeneity of the injected plasma was studied in zero electric and magnetic field by observing the transmission of a focused 17-μ Ne laser beam, as shown in Fig. 1. A cell filled with a variable pressure of SF_6 gas was used to vary the intensity of the 10.6-μ beam without displacing the focus in the sample. The 10.6-μ radiation was focused on the sample with a 20-cm focal length BaF_2 lens so that the focal region in the sample was uniform over lengths of the order of a 1 cm. The focal diameter was about 0.3 mm. A 17-μ Ne laser beam was focused with a 5-cm focal length KRS-5 lens to a focal diameter of the order of 100 μ, and the absorption of this beam appeared as a dip in transmitted 17-μ, signal monitored on a liquid-helium-cooled Cu-doped Ge detector. The sample was mounted on a liquid-nitrogen-cooled cold finger and its temperature was estimated as 100°K. The back face of the sample was cut at an angle to eliminate the reflected beam. It is interesting to note that a "negative" signal is seen at the detector even when the Ne laser is blocked. This is caused by a decrease in the amount of room-temperature blackbody radiation reaching the detector, because of the absorption of the cold injected plasma. This signal was minimized by a cold shield with a narrow aperture for the 17-μ probe beam.

The absorption at 17 μ is primarily caused by the relatively large hole absorption coefficient [Eq. (4)] and is directly proportional to the free-hole concentration. We assume that the free-hole and -electron concentrations are equal, i.e., that the traps are saturated and bimolecular recombination predominates. This assumption is supported by the observation that both

[16] A. F. Gibson, M. J. Kent, and M. F. Kimmitt, Brit. J. Appl. Phys. **1**, 149 (1968).
[17] R. Braunstein, Phys. Rev. **125**, 475 (1962).
[18] L. V. Keldysh, Zh. Eksperim. i Teor. Fiz. **47**, 1945 (1964) [English transl.: Soviet Phys.—JETP **20**, 1307 (1965)].
[19] I. Melngailis and R. H. Rediker, Proc. IRE **50**, 2428 (1962).

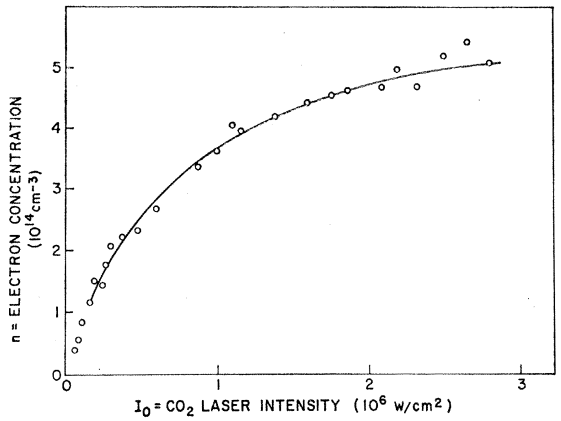

FIG. 2. Injected electron-hole plasma density as a function of incident CO_2 laser intensity as measured by absorption of 17-μ radiation $\sim$2 mm from the face on which the 10.6-μ radiation is incident.

recombination radiation and the absorbed 17-μ signal follow the laser signal. Thus, the peak absorption of the 17-μ radiation is taken as a direct measure of both electron and hole concentrations. The intensity dependence of the peak 17-μ absorption is shown in Fig. 2, with the 17-μ focus $\sim$2 mm from the face on which the 10.6-μ radiation is incident. This concentration dependence on laser intensity can be explained with the rate equation

$$\begin{aligned} &\partial n/\partial t + rn^2 - cI^2 = 0, \\ &W_L = cI^2, \end{aligned} \tag{5}$$

where n is the electron concentration (assume $n \simeq p \gg n_0$, p_0), r is the recombination rate, c is the two-photon creation rate, and I is the 10.6-μ laser intensity. Since the recombination radiation follows the incident pulse we assume

$$rn^2 \gg \partial n/\partial t, \tag{6}$$

and since hole absorption is dominant,

$$dI/dx = -\sigma_p n I. \tag{7}$$

Then we obtain

$$n(x,I_0) = \frac{I_0}{I_0 x \sigma_p + (r/c)^{1/2}} = \frac{1}{\sigma_p x + n(0)^{-1}}, \tag{8}$$

where I_0 is the incident 10.6-μ intensity at $x=0$, and

$$n(0) = (c/r)^{1/2} I_0 = [W_L(0)/r]^{1/2} = W_L(0)\tau_R(0) \tag{9}$$

is the injected concentration at $x=0$, and

$$\tau_R(x) = 1/n(x)r \tag{10}$$

is the recombination time. The solid curve in Fig. 2 shows a least-squares fit to Eq. (8), with $\sigma_p x \simeq 1.6\times10^{-15}$ cm^3 and $n(0) \cong 10^{15}$ cm^{-3} for $I_0 \simeq 1\times10^6$ W/cm^2. If we take a measured[20] value of $\sigma_p \simeq 5\times10^{-15}$ cm^2, we obtain $x \simeq 0.32$ cm, which is in order-of-magnitude agreement with the measured distance of 0.2 ± 0.05 cm. Similar saturation curves were obtained at 1-mm intervals along the sample and the fitted parameters were all within a factor of 2 of those obtained from Fig. 2. In this regard, the simple rate-equation approach seems to work well. However, the values of $n(0)$ obtained from the above analysis are nearly two orders of magnitude smaller than those estimated in the introduction. The values of I_0 may be high since it is difficult to determine the actual beam geometry in the focus at the sample and the value of n measured by 17-μ absorption is uncertain with a factor of 2. The radiative recombination rate was estimated[21] from Kane's calculation[22] of the dipole matrix element in InSb and Dumke's[23] average of transition probability; thus, $r \simeq 2\times10^{-7}$ cm^3 sec^{-1}. I_0 of 5×10^5 W/cm^2 corresponds to an E_L in the sample of $\sim10^4$ V/cm, and using the Keldysh[1] or Braunstein estimates of W_L one obtains the estimate in Eq. (1). The weakest link in this chain of estimates is probably the value of r, since there may be a sizeable contribution from nonradiative recombination. Since a major fraction of the incident power is absorbed in the first 10–100 μ of the sample (if $I_0 > 10^6$ W/cm^2), appreciable heating may occur, and Auger recombination may make a significant contribution. The hole thermalization time[24,25] of $\sim10^{-11}$ sec (electrons thermalize in $\sim10^{-7}$ sec independently, but since their hole collision time is $\sim10^{-13}$ sec they will thermalize with the holes) probably maintains the plasma temperature equal to the

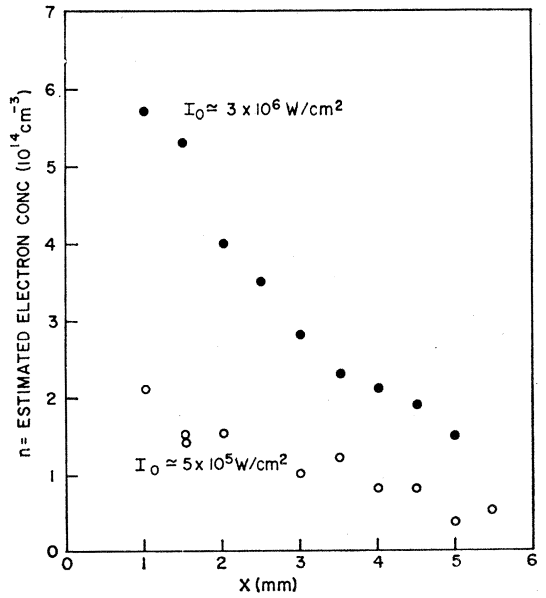

FIG. 3. Plasma density as a function of a distance x from 10.6-μ-incident surface for two fixed intensities.

[20] S. W. Kurnick and J. M. Powell, Phys. Rev. **116**, 597 (1959).
[21] B. Ancker-Johnson, in Proceedings of the International Semiconductor Conference, Moscow, 1961 (unpublished).
[22] E. O. Kane, J. Phys. Chem. Solids **1**, 249 (1957).
[23] W. P. Dumke, Phys. Rev. **105**, 139 (1957).
[24] G. D. Peskett and B. V. Rollin, Proc. Phys. Soc. (London) **82**, 467 (1963).
[25] S. M. Kogan, Fiz. Tverd. Tela **4**, 2474 (1962) [English transl.: Soviet Phys.—Solid State **4**, 1813 (1963)].

lattice temperature; thus, the temperature rise is constrained by the specific heat of the lattice. A rough estimate shows a temperature rise of the order of 10^2–10^3°K for a 10-kW beam focused to a 100-μ spot. This surface heating caused by hole absorption may also explain the surface sparking that is often observed for $I_0 \geq 10^7$ W/cm^2. Another lifetime mechanism that is changed by the presence of the high-intensity beam is the trapping lifetime.[16] The laser photon energy is sufficient to ionize and populate traps. However, since the trap density is probably less than 10^{14} cm^{-3}, traps can be considered saturated for plasma densities much greater than 10^{14} cm^{-3}.

Figure 3 shows the spatial density variations at two fixed 10.6-μ intensities. The plasma density estimated from Eq. (8) saturates at $(\sigma_p x)^{-1}$ for the region investigated. This limit probably is valid for the 3×10^6 W/cm^2 data, since we know from Fig. 2 that saturation has been reached. However, the measured density decreases by a factor of $\sim$3 for a decrease in laser intensity of $\sim$6. This again indicates an error in the estimate of W_L, r, or I_0. By using a reflector on the back surface or by irradiating the sample from two opposite directions, one should be able to obtain homogeneous plasma densities of $\sim10^{15}$ cm^{-3} within a 1-mm cube.

C. Recombination Radiation

Recombination radiation near 5.3 μ was easily seen from the injected plasma. When the sample was immersed in liquid He the recombination radiation spectral width was $\sim$10 cm^{-1}, indicating a plasma temperature of less than 10°K.[26] The recombination radiation pulse was no longer than the laser pulse, indicating a recombination time of $<$0.1 μsec. The samples could be mounted on a parabolic reflector in the bore of a superconducting solenoid, which produced fields up to 55 kOe. The field dependence of the integrated recombination radiation power is shown in Fig. 4 for both 9.6 and 10.6 μ. n- and p-type InSb gave similar results.

CO_2 laser radiation at 10.6 and 9.6 μ corresponds to photon energies of 0.117 and 0.128 eV, respectively. As multiples of these energies become equal to the energy difference between the valence band and the relatively widely spaced Landau levels of the conduction band, peaks in the recombination radiation occur corresponding to an increase in the multiphoton absorption process.[3] At 10.6 μ only one peak occurs corresponding to the $l=0$ Landau level, and at higher fields the radiation decreases to $\sim$8%, where it remains relatively constant, probably because of three photon absorption, excitation via traps, impurity bands, and phonon assisted transitions. Peaks corresponding to three photon absorption can be seen in the 10.6-μ photoconductivity (see Fig. 7). At 9.6 μ the peaks are periodic in $1/B$ and the peak with spin splitting at

[26] A. Mooradian and H. Y. Fan, Phys. Rev. 148, 873 (1966).

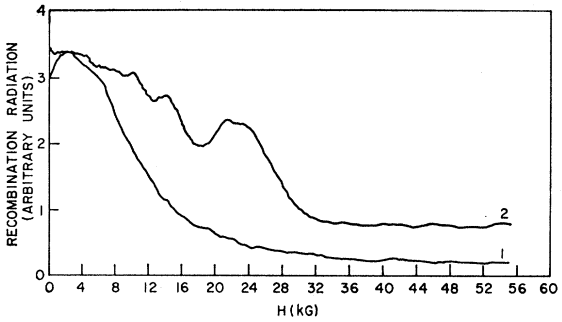

FIG. 4. Recombination radiation from multiphoton-injected plasma as a function of magnetic field for 9.6-μ (curve 2) and 10.6-μ (curve 1) exciting radiation. Sample temperature was 4.2°K.

$\sim$23 kOe corresponds to the $l=1$ Landau level. The $l=0$ level peak for 9.6 μ should occur at 63 kOe. These peaks are similar to those observed in Shubnikov–de Haas oscillations where the Fermi level crosses the Landau levels. However, the peaks observed here and in Sec. D below are independent of laser intensity and thus are not connected with the Fermi level.

D. Multiphoton Conductivity

The photoconductivity of a n-InSb bar $2\times2\times3$ mm was measured with the sample immersed in liquid nitrogen (LN_2) and liquid helium (LHe) in the bore of a superconducting solenoid. The In end contacts

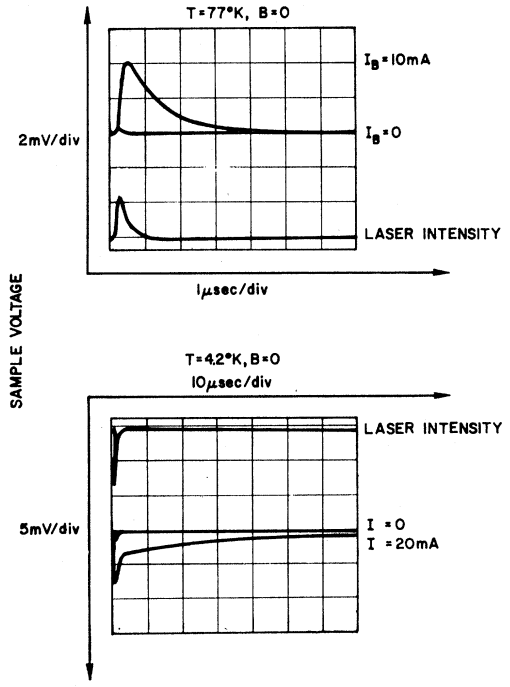

FIG. 5. Photoconductivity response of n-InSb from plasma injected by 10.6-μ CO_2 laser pulse with peak power of $\sim10^4$ W/cm^2 at LN_2 and LHe temperatures. I_B is the constant current through the sample.

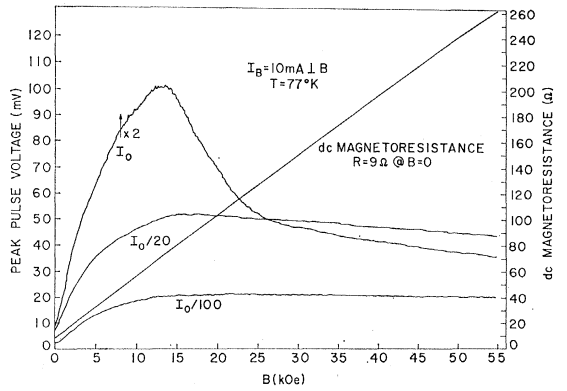

FIG. 6. Magnetic field dependence of photoconductive signals in n-InSb ($n_0 \sim 5\times10^{13}$ cm^{-3}) at LN_2 temperatures. I_0 at 10.6 μ was $\sim10^5$ W/cm^2. Peak voltage was measured perpendicular to both magnetic field and laser direction.

were shielded with Al foil to avoid photovoltaic response. The laser radiation was filtered to allow only 10.6-μ radiation on the sample. Conductivity was measured using a constant-current source and the signal induced by the laser was fed by matched coax cable to the oscilloscope and boxcar integrator. Figure 5 shows oscilloscope traces of the time-resolved laser pulse and photoconductivity pulses at LN_2 and LHe. First notice that there are signals at both temperatures in the absence of a bias current.[27] These signals are not well understood at present, but they must result from an inhomogeneity of the beam intensity or the sample. The sign of this signal was independent of the beam position on the sample and laser mode configuration. Inhomogeneities caused by strain or back-reflected laser light were not eliminated as possible causes. These zero bias signals follow the time dependence of the laser in great detail and vary nonlinearly with laser intensity.

The photoconductive response with a constant-current source is

$$V_s=[I_B l/2A\sigma(0)][1-\sigma(0)/\sigma], \tag{11}$$

where the conductivity σ for n-type material is

$$\begin{aligned}\sigma&=(n_0+n)eb\mu_h+pe\mu_h,\\ \sigma(0)&=n_0eb\mu_h,\end{aligned} \tag{12}$$

where l is the length of the sample, A is the cross-sectional area of the laser beam, n and p are the laser-induced electron and hole densities, b is the mobility ratio ($\sim$36 for InSb), μ_h is the hole mobility, and $n_0\sim5\times10^{13}$ cm^3 is the donor electron concentration. For n, $p\ll n_0$, the measured voltage V_s varies linearly with n and p; however, for n, $p\gg n_0$, V_s saturates and varies as $(1-n_0/nb+p)$. This saturation could be observed at $I_0\simeq10^5$ W/cm^2 at both LN_2 and LHe temperature. Relaxation rates are difficult to interpret in this saturated region so that no details of the dynamics of the plasma with n, $p>n_0$ were obtained. This region might best be investigated with a constant-voltage arrangement but it would be difficult to eliminate the relatively high resistance of nonirradiated positions of the sample.

At LN_2 temperatures Fig. 4 shows an exponential decay of conductivity which indicates a monomolecular decay of a single carrier. This is probably the holes being trapped, since the time constant is in good agreement with the measurements of Laff and Fan[28] at this temperature. An order-of-magnitude increase in I_0 produced a saturated behavior as predicted by Eq. (11), and the decay became more nearly linear as expected for bimolecular recombination in the region where traps are saturated (n, $p\geq10^{14}$ cm^{-3}).

The magnetic field dependence of the peak of the photoresponse at LN_2 temperature is shown in Fig. 6. Since the magnetoresistance increases nearly two orders of magnitude from 0 to 55 kOe the applied electric field varies from 0.1 to 10 V/cm. At low laser intensities the response was independent of I_B up to 10 mA. The photoresponse normalized for the change in magnetoresistance shows a peak at $\sim$3 kOe, where the two-photon injection is expected to peak since the valence to conduction band gap energy becomes equal to twice the laser photon energy. The normalized response at 55 kOe is $\sim$1/50 of the zero-field response, in rough agreement with the recombination radiation results of Fig. 4. For incident intensities of $I_0/20$ and I_0 the behavior is nearly saturated, i.e., p, $n\geq n_0$. At the maximum intensity the field dependence of the photoresponse differed from the lower intensities and showed a sharp drop in the region from 5 to 20 kOe. At times the drop was accompanied by sharp peaks and very unstable behavior from pulse to pulse, indicating an instability of the injected plasma. The time response of the photoconductivity did not change appreciably ($<20\%$) as a function of the applied magnetic or electric field. Longitudinal photoconductive response was similar to that shown in Fig. 6.

At liquid-helium temperatures several features of the photoconductivity changed. First the time response shown in Fig. 5 has two components, one that follows the laser pulse and saturates at $I_0>10^5$ W/cm^2 and a long tail which is probably caused by the trapping of holes at densities below 10^{14} cm^{-3}. The decay constant in the tail varied $\leq$10–20% as B or the applied electric field was varied (decreased for increasing E and increased for increasing B). The magnetic field dependence shown in Fig. 7 was much more sensitive to applied electric field than at LN_2. Twice the laser photon energy, 0.234 eV, falls just at the edge of the main gap absorption at 4.2°K[17]; thus, the peak at 0 kOe is probably caused by the band-to-band two-photon absorption and the peak at 3–4 kOe may be caused by populating and

[27] Similar signals have been observed in doped semiconductors. C. K. N. Patel and R. E. Slusher, also J. H. McFee and N. Van Tran (private communication).

[28] R. A. Laff and H. Y. Fan, Phys. Rev. **121**, 53 (1961).

ionizing an impurity band. Since the position of this peak varies with incident intensity, it may indicate heating of the sample at the incident face. At higher fields the series of peaks corresponds to three times the laser photon energy, equaling the valence-band–to–Landau-level separation.[3] These three-photon absorption peaks were seen only when the peak of the photoresponse was monitored. For $I_0 \approx 10^5$ W/cm^2 the saturation region is attained; however, no instability similar to those at LN_2 temperatures was observed at LHe.

III. SUMMARY

These preliminary measurements of properties of multiphoton-injected plasmas indicate several interesting areas for further research. First, it seems possible to inject homogeneous plasmas with densities in the 10^{15}-cm^{-3} range, whose temperatures are very close to the lattice temperature down to at least 10°K. These field-free injected plasmas should be of considerable interest in studying plasmas instabilities in InSb. Some recent results[29] indicate interesting interactions between the laser-injected plasma and an electric-field-injected plasma. Shorter CO_2 laser pulses may be able to probe the plasma lifetimes in more detail, using the recombination radiation and constant-voltage photoconductivity as indicators. It is also possible to produce dense ($>10^{14}$ cm^{-3}) plasma in magnetic fields up to 100 kOe using both 9.6- and 10.6-μ radiation with intensities in the range above 10^5 W/cm^2.

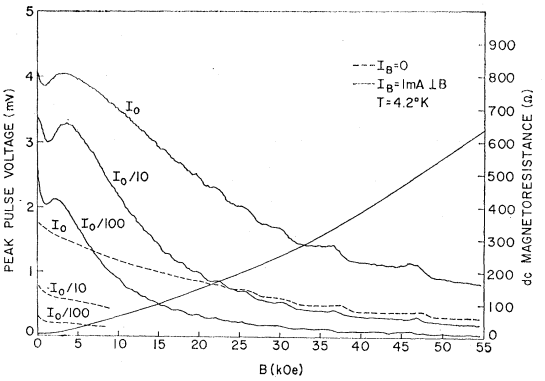

FIG. 7. Magnetic field dependence of peak photoconductive signal during 10.6-μ laser pulse for n-InSb at LHe temperature. Other parameters are similar to those in Fig. 6.

ACKNOWLEDGMENTS

We would like to thank B. Ancker-Johnson, C. K. N. Patel, and P. A. Wolff for helpful discussions, and J. Strautins for technical assistance.

[29] R. Slusher, W. Giriat, and B. Ancker-Johnson (unpublished).

PHYSICAL REVIEW VOLUME 183, NUMBER 3 15 JULY 1969

Calculation of the Reflectivity, Modulated Reflectivity, and Band Structure of GaAs, GaP, ZnSe, and ZnS†

JOHN P. WALTER* AND MARVIN L. COHEN
Department of Physics and Inorganic Materials Research Division, Lawrence Radiation Laboratory, University of California, Berkeley, California 94720

(Received 13 January 1969)

We have calculated the electronic energy band structure, the imaginary part of the frequency-dependent dielectric function, the reflectivity, and the modulated reflectivity (derivative of the reflectivity) for GaAs, GaP, ZnSe, and ZnS, using the empirical pseudopotential method. A direct comparison of the measured and calculated reflectivities is made. The calculated derivative of the reflectivity spectrum is compared with thermoreflectance data.

INTRODUCTION

THE electronic energy-band structure has been calculated by us; also, the imaginary part of the frequency-dependent dielectric function $\epsilon_2(\omega)$; the reflectivity $R(\omega)$; and the modulated reflectivity $R'(\omega)/R(\omega)$, where $R'=dR/d\omega$, for GaAs, GaP, ZnSe, and ZnS, using the empirical pseudopotential method[1] (EPM). In previous calculations[2] the imaginary part of the frequency-dependent dielectric function $\epsilon_2(\omega)$ was calculated and compared with experiment. However, since the reflectivity is the actual quantity measured, it was felt that a direct comparison between measured and theoretically calculated reflectivity would be desirable. The main reason for wanting a comparison of this type rather than an $\epsilon_2(\omega)$ comparison is that it is necessary to use an integral transform of the reflec-

† Work supported in part by the National Science Foundation.
* National Science Foundation Graduate Fellow.
[1] M. L. Cohen and T. K. Bergstresser, Phys. Rev. 141, 789 (1966), and references therein.
[2] W. Saslow, T. K. Bergstresser, C. Y. Fong, M. L. Cohen, and D. Brust, Solid State Commun. 5, 667 (1967).